



Research paper

Phosphoranimes containing cationic N-imidazolium moieties

John R. Klaehn^{a,*}, Harry W. Rollins^a, Joshua S. McNally^a, Navamoney Arulsamy^b, Eric J. Dufek^c^a Biological and Chemical Processing, Idaho National Laboratory, P.O. Box 1625, Idaho Falls, ID 83415-3732, USA^b Department of Chemistry, University of Wyoming, 1000 E. University Ave, Dept 3838, Laramie, WY 82071, USA^c Energy Storage and Advanced Vehicles, Idaho National Laboratory, P.O. Box 1625, Idaho Falls, ID 83415, USA

ARTICLE INFO

Article history:

Received 20 April 2017

Accepted 31 May 2017

Available online 1 June 2017

Keywords:

Synthesis

Characterization

Phosphoranime

X-ray crystal structure

Room temperature ionic liquid

ABSTRACT

Three new monomeric phosphoranimes (PAs; $R-N=PR_3$) were synthesized by the Staudinger route using 2-azido-1,3-dimethylimidazolium hexafluorophosphate [ADMImPF] and various phosphines to form their respective PA salts of triphenylphosphine (**1**), tri(*n*-octyl)phosphine (**2**), and tris(2,2,2-trifluoroethoxy)phosphite (**3**). These PA salts have a cationic imidazolium moiety attached to nitrogen. Interestingly, **2** is a room temperature ionic liquid (RTIL) with a melting point around $-5\text{ }^\circ\text{C}$ and a viscosity of 740cP at $25.5\text{ }^\circ\text{C}$. **1** and **2** show stability to moisture exposure and atmosphere for weeks whereas **3** is not stable toward atmospheric moisture undergoing decomposition to form 2-amino-1,3-dimethylimidazolium phosphate (**4**). Thermal analyses reveal that **1** and **2** are stable to $90\text{ }^\circ\text{C}$ under nitrogen, but **3** undergoes degradation by exposure to moisture and/or elevated temperature. All compounds exhibit similar multinuclear NMR chemical shifts as compared to their corresponding phosphine oxide counterparts. However, their respective X-ray structure determinations indicate that **2** has an open structure with the octyl groups that avoid the ionic charges, whereas **1** and **3** have tighter structural packing of the hexafluorophosphate to their pendant groups.

© 2017 Published by Elsevier B.V.

1. Introduction

Phosphoranimes (PAs; Fig. 1) are small molecule phosphorus-nitrogen compounds that are common building blocks to make polyphosphazenes or cyclic phosphazenes [1–4]. These materials have unique properties that range in a variety of membrane, biological, and electronic applications [5–8], and recently PAs were shown that they could be used as an additive battery electrolyte in lithium-ion batteries [9]. Traditional PA chemistry has been used to generate polymeric phosphazenes, where the PAs contain a trimethylsilyl-group at nitrogen (Fig. 1) and different phosphorus pendant groups, such as directly bound alkyl/aryl groups and a good leaving group (chloro-, trifluoroethoxy- or phenoxy-) [3,7,10–12]. Generally, heating these PAs to $180\text{--}200\text{ }^\circ\text{C}$ results in condensation polymerization, and recent literature has shown that some of their oligomeric intermediates can be isolated as ionic moieties even at ambient temperatures in the presence of Lewis acid catalysts (e.g., PCl_5) [13–16]. This polymerization has been studied to determine the reactive intermediate compound (ionic PA) that sustains the living polymerization at ambient temperatures [15,16]. Several different ionic PA intermediates were charac-

terized; however, the resulting ionic PAs are not stable towards atmospheric moisture and will tend to degrade. Other PA compounds with a reactive imide ligand (hydrogen, halogen or organosilane) can be transformed into a reactive intermediate that builds larger PA structured compounds and metal complexes, such as the aza-Wittig reagents [17–23]. Interestingly, recent research has shown similar ionic and non-ionic PA compounds can be used for polymerization and depolymerization catalysts/co-catalysts of various organic condensation polymers, e.g. depolymerization of polyesters using sterically hindered, strong PA Lewis bases [24–26,21].

Most PAs without a P=N-P backbone (only P=N) structure are made by two common synthetic strategies: Neilson method or Staudinger reaction [3,11,27–30]. The Neilson method is the preferred synthetic route in making PA precursors, as it avoids the use of hazardous organic azides, as well as the creation of unwanted by-products through P=N cyclization, and limits phosphite or PA rearrangement products, such as alkyl phosphoramidates $((\text{RO})_2\text{P(=O)NH}_2)$ [11,30,31]. The disadvantage of the Neilson method is that it requires several reaction steps followed by vacuum distillation to achieve a pure PA product. Also, because the method produces products that tend to polymerize to yield polyphosphazenes, the Neilson method is limited to producing moisture sensitive PAs with organosilanes at nitrogen. As the

* Corresponding author.

E-mail address: john.klaehn@inl.gov (J.R. Klaehn).

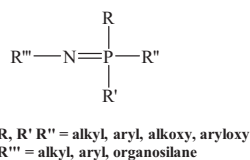


Fig. 1. N-organophosphoranimine (PA) structure.

oldest synthetic route to PAs, the Staudinger route comprises of a single step reaction between an azide and phosphine where a variety of N and P pendant groups can be utilized to make unique PA compounds.

Over the past decade, new interest in the Staudinger reaction has re-emerged through “click” chemistries, such as azide fluorescent markers on biological materials or attachments to polymer pendant groups [32–35]. Several new organic azides from commercial sources not only can be utilized for the Staudinger 3+2 “click” reactions, but they can also be used with phosphines to make new PAs. In some cases, these organic azides are stable as purified solids, e.g. 2-Azido-1,3-dimethylimidazolium hexafluorophosphate [ADMImPF] [36–38]. ADMImPF can be used directly in the Staudinger reaction without needing to employ rigorous safety precautions during the synthesis. The added azide stability is essential to the Staudinger method and introduces new PA compounds which are not easily accessible by the Neilson method. We report three cationic N-imidazolium PA compounds that were synthesized from the reactions of triphenylphosphine (TPP), trioctylphosphine (TOP) or tris(2,2,2-trifluoroethoxy)phosphite (TTFP) with ADMImPF. All isolated PA products were characterized by multinuclear NMR and single crystal X-ray diffraction, and the thermal properties and reactivity towards the atmosphere and moisture were also characterized.

2. Results and discussion

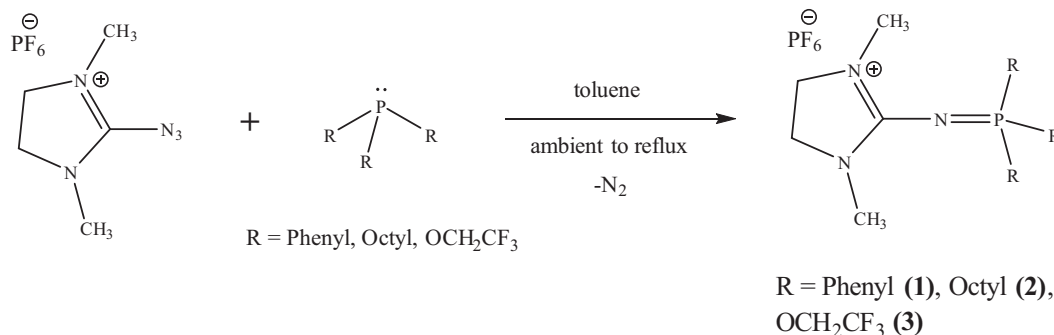
A series of monomeric PA salt products (Scheme 1 and Fig. 2) with an organophosphine (TPP, TOP or TTFP) and ADMImPF were synthesized by the Staudinger method: P,P,P-triphenylphosphoraniminyl-N-1,3-dimethylimidazolium hexafluorophosphate [1], P,P,P-trioctylphosphoraniminyl-N-1,3-dimethylimidazolium hexafluorophosphate [2], and P,P,P-tris(2,2,2-trifluoroethoxy)phosphoraniminyl-N-1,3-dimethylimidazolium hexafluorophosphate [3]. These PA compounds can be a solid or liquid at room temperature, depending on the pendant groups at phosphorus. PA 2 was the most interesting due to it being an atmospherically stable room temperature ionic liquid (RTIL) with a viscosity of 740cP (25.5 °C). Previous PA compounds by the Neilson and Staudinger synthetic methods focused on attaching or creating ionic moieties at the phosphorus position, such as imidazolium halides, organophosphines, and

4-dimethylaminopyridine [39–42]; however, their PA products are not commonly stable under atmospheric conditions for extended periods. Also, there are a limited number of usable organic azide compounds, and the syntheses of PA compounds with a cationic pendant group at nitrogen have not been explored by the Staudinger method. In the literature, atmospherically stable PA compounds are formed as either (large) sterically encumbered alkyl/aromatic PA compounds [11,43,44] or as various forms of ionic aromatic structures of $\text{Ph}_3\text{P}=\text{N}^+=\text{PPh}_3 \text{X}^-$ ([PPN]Cl) with halogen anions [20,42,45], giving the [PPN]Cl structure its stability and its charge distribution across the compound. Hence, the reported compounds 1–3 have the ability to distribute the charge across the PA structure through electron resonance structures (Fig. 3), which can enhance their stability for extended periods.

ADMImPF is a commercial product that is available as a white powder. It is stable to brief exposure to the atmosphere at room temperature. Thus, it is relatively simple to handle in the laboratory and a good candidate for the Staudinger reaction. Even though, ADMImPF is not completely soluble in toluene (as reported in the literature), the reported phosphines were able to react with the azide in toluene without issues. In addition, toluene allowed for easier workup and has a useful temperature range for these reactions.

All three new PAs form a yellow colored intermediate during reaction. 1 and 2 show distinct color changes that dissipated over time as the azide reacted with the phosphine. It is interesting that all three reactions do not proceed at room temperature do not immediately react as the phosphine was added, but further heating was required to yield PA products, such as 2 and 3. All PA products were not completely soluble in toluene and tend to precipitate or oil out of solution upon cooling to room temperature. Also, these compounds do not show water solubility. The toluene solution was decanted or pipetted away from the products, where they were washed and isolated from hexane solutions. The PAs that are solids could be purified further by common recrystallization methods. In the instance of synthesizing compound 2, isolation was carried out using hexanes, and the compound remained as an oily liquid at room temperature after solvent removal. This product was placed in a freezer (−30 °C), where prismatic crystals were generated. All of the reported PA products were isolated and analyzed by multi-nuclear NMR, thermal analysis, and single-crystal X-ray diffraction.

In Table 1, the multi-nuclear P-31 NMR spectra of 1–3 show that $\text{CF}_3\text{CH}_2\text{O}$ groups contribute more electron density to phosphorus than the phenyl or octyl groups. When comparing compounds 1–3 to their phosphine oxide precursors [46], all compounds follow similar trends in the chemical shifts; however, PAs 1–3 have slightly more electron density at phosphorus resulting in a 12–17 ppm upfield shift. No differences in chemical shifts are observed among the P-31 NMR spectra of the PF_6^- counter ion to compounds 1–3, which would be expected due to the over-



Scheme 1. Staudinger reaction of 2-azido-1,3-dimethylimidazolium hexafluorophosphate (ADMImPF) and phosphines to form PA compounds 1–3.

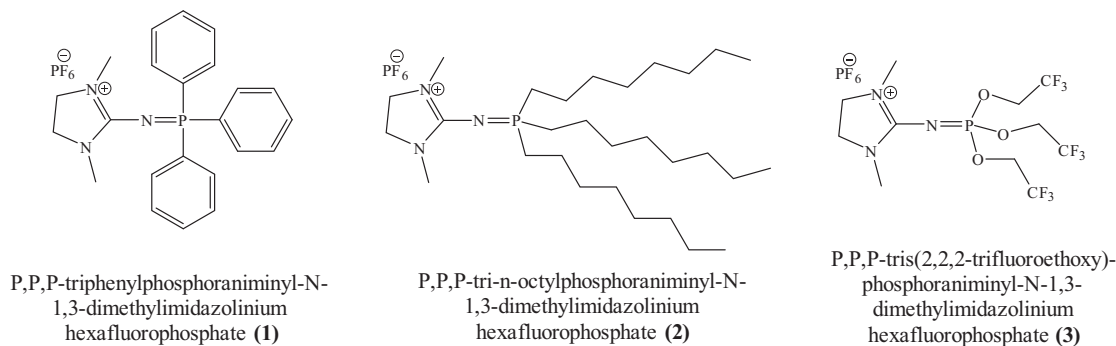


Fig. 2. PA structures of compounds 1–3.

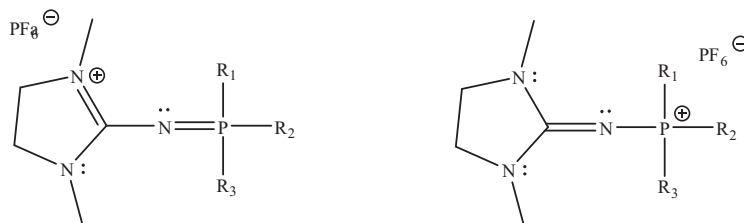


Fig. 3. Potential ionic resonance structures of the imidazolium PA compounds.

Table 1

P-31(¹H) NMR Chemical Shifts (δ in ppm) of Ionic PAs 1–3 and their respective P-31 (¹H) NMR Chemical Shifts of phosphine oxides (relative to 85% H₃PO₄).

R=	OCH ₂ CF ₃ [3]	Ph [1]	n-Octyl [2]
Ionic PA ¹	–14.8 (s)	13.0 (s)	31.7 (s)
R ₃ P=O ²	–2.8 (s)	27.0 (s)	48.5 (s)

¹ This work.

² Ref. [46].

whelming influence of local fluorines. Since **3** was not found to have long term stability under atmospheric conditions, exposure testing was only performed on **1** and **2**. These exposure tests were conducted in moisture conditions (~10 wt% water in d₈-THF; Figs. 4–7), and they were analyzed by P-31 and F-19 NMR to see if any degradation products of the PA or PF₆ were produced over a period of several weeks. Over this time period, no detectable aqueous decomposition products, which are phosphine oxides from **1** and **2** and hydrofluoric acid formation from PF₆[–], are observed in **1** for either the P-31 or F-19 NMR spectra after 14 days. But, **2** showed a small amount of phosphine oxide that increased from 0.6% (initial) to 2.3% (29 days) by integration in P-31 NMR (upper left in Fig. 6), and no observable changes in the F-19 after 30 days. These NMR spectra show that water exposure is not an immediate issue with **1** and **2** under these conditions; however, further studies will have to be performed to understand if these compounds can be used in more aggressive conditions (temperature, acidic pH, etc.). Overall, the combined results of exposure to water and atmospheric conditions indicate that some of these ionic PA products can be exposed for long periods without decomposing at ambient conditions. This is important for RTILs, such as **2**, which could be used in aqueous/organic solvent conditions.

Determination of melting points and/or degradation temperatures for these ionic PA compounds was performed using differential scanning calorimetry (DSC; see Figs. 8–10). All thermal scans were cooled down to –80 °C and held for 30 min to ensure that the compounds were solids and at thermal equilibrium prior to determining their melting points. PA **1** showed a melting point at about 185 °C and crystallization at about 145 °C upon the cooling

return of the scan. There is a slight difference in the melting point between the two DSC runs, but the crystallization showed the same temperature. PA **2** is the RTIL that showed a small broad melting point at –5 °C that remained after the first heating cycle. The interesting point is that the compound does not show a crystallization point on the cooling return of the DSC, but it does solidify during the 30-min hold at –80 °C, which might flash-freeze the compound (amorphous solid structure) to give a large –65 °C melting point. The inflection points prior to the melting point could be due to some variation in the crystalline and amorphous solid structures of **2**. Data for PA **3** indicates that the compound decomposed upon exposure of the atmosphere. When using the melting point apparatus, crystals of **3** show a melting point at 97–98 °C; however, the DSC indicates two different compounds were present that had melting points at –45 °C and at 95 °C. The two melting points indicate that **3** is not stable under atmospheric conditions or in thermocycling. Scheme 2 illustrates a possible degradation pathway that yields the imidazolium hexafluorophosphate and the organophosphate(s). The resulting imidazolium salt, 2-amino-1,3-dimethylimidazolium hexafluorophosphate (**4**), was later identified by X-ray crystallography (see crystallographic data). The CF₃CH₂O– groups are known as good leaving groups for the PA condensation polymerization; therefore, it is reasonable to assume that decomposition of PA **3** initiates with loss of trifluoroethoxide. In addition, the X-ray structure of PA **3** could not be well resolved as it crystallizes out as clusters of thin plates, which did not yield the highest quality crystals. Consequently, the structural parameters are less accurately determined. The data, however, can be considered as reasonable approximation of the parameters. Crystallographic data collection and refinement parameters are given in Table 2, and selected structural data are collected in Table 3.

In contrast, the crystallographic structures of **1** and **2** are well refined. These structures together with that of PA **3** provide evidence that ion pairing is observed with the imidazolium nitrogens or phosphorus (see Fig. 3), but this might be due to crystal packing. From Fig. 3, there is a possibility of a resonance structure in these PA compounds where the positive charge can be distributed from the imidazolium nitrogens to phosphorus.

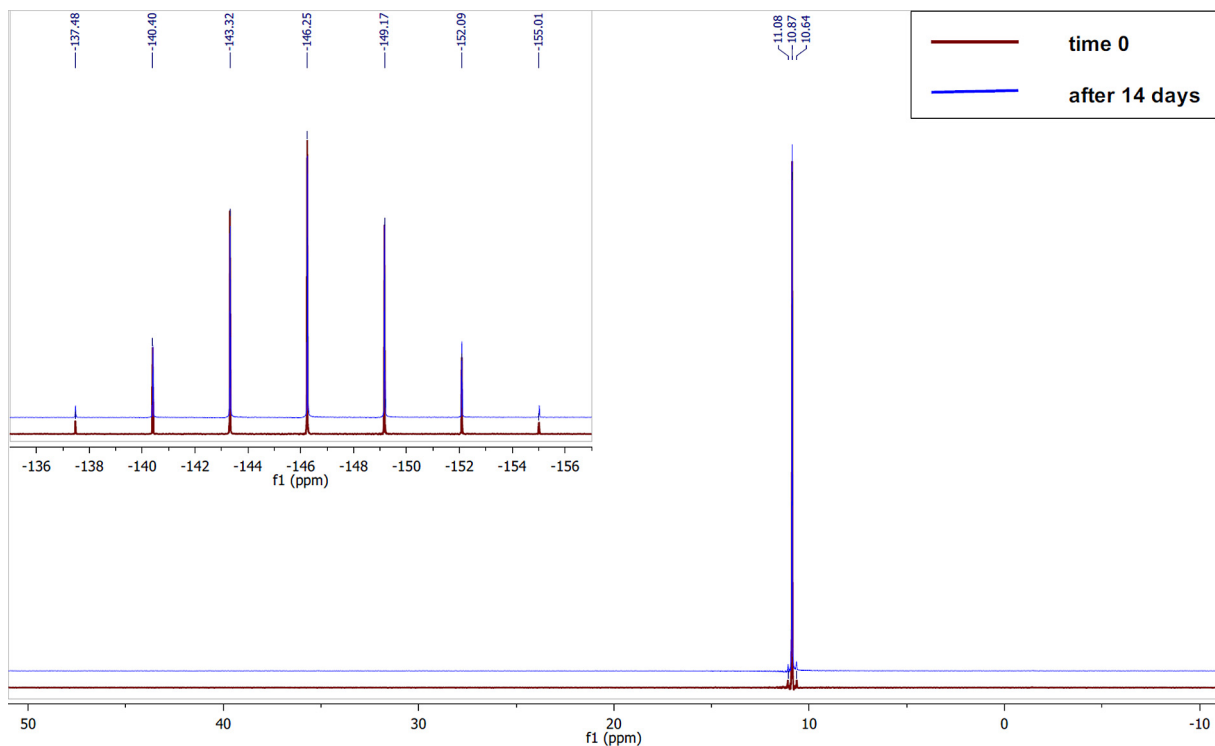


Fig. 4. P-31(¹H) NMR Spectra of **1** and PF₆ (upper left) for 14 days.

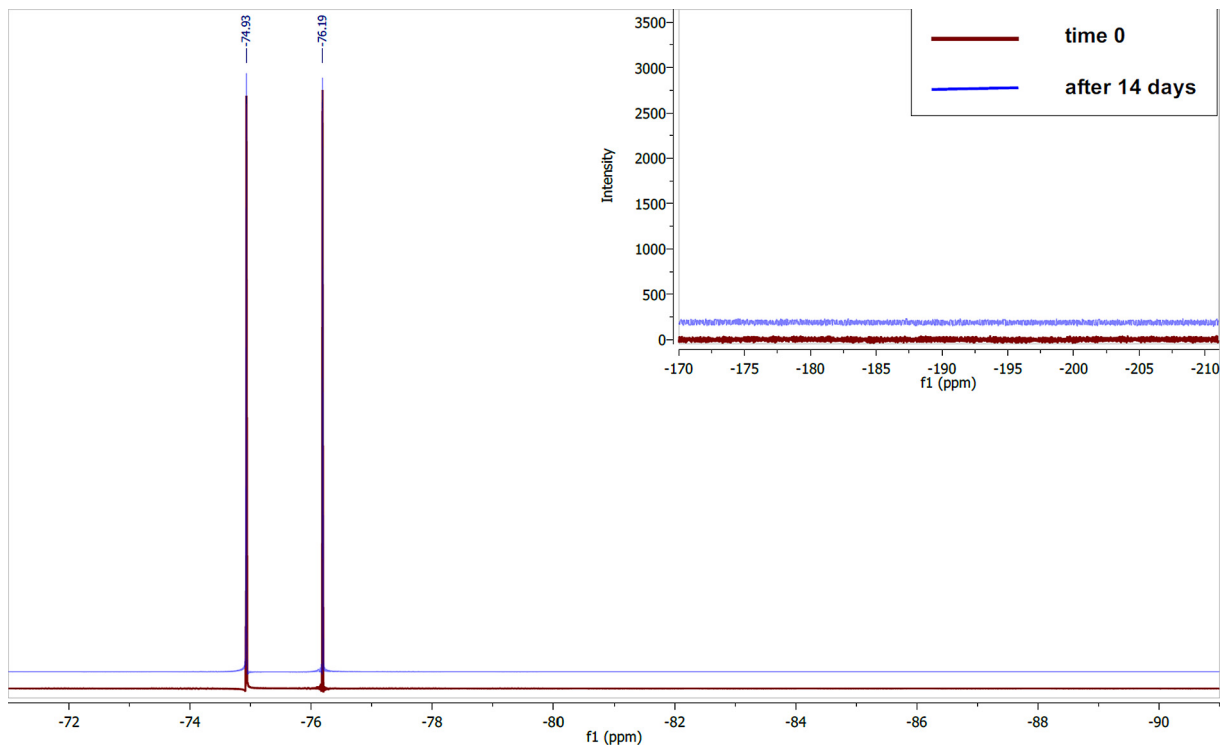


Fig. 5. F-19(¹H) NMR Spectra of **1** and HF (upper right) for 14 days.

The P-31 NMR spectra (Fig. 6) show an electron poor phosphorus center containing the octyl groups (**2**), and the phosphorus center becomes more electron rich when phenyl (**1**) and alkoxy groups (**3**) are bound to phosphorus. However, when comparing the PA electron density between their P-31 NMR spectra and the location of the PF₆⁻ anion to in the X-ray structures (Figs. 11–16), there

is no clear spectral trend with the location of the PF₆⁻ anion and the PA phosphorus center. Even from the X-ray structural data, the ionic bond distances between the nitrogen atoms of the imidazolium cations and PF₆⁻ anions are at 3.456(1), 3.163(4) and 3.273 (9) Å, respectively in **1–3**. The PF₆⁻ anions are within 0.3 Å in proximity, indicating all have similar ionic interactions. As shown in

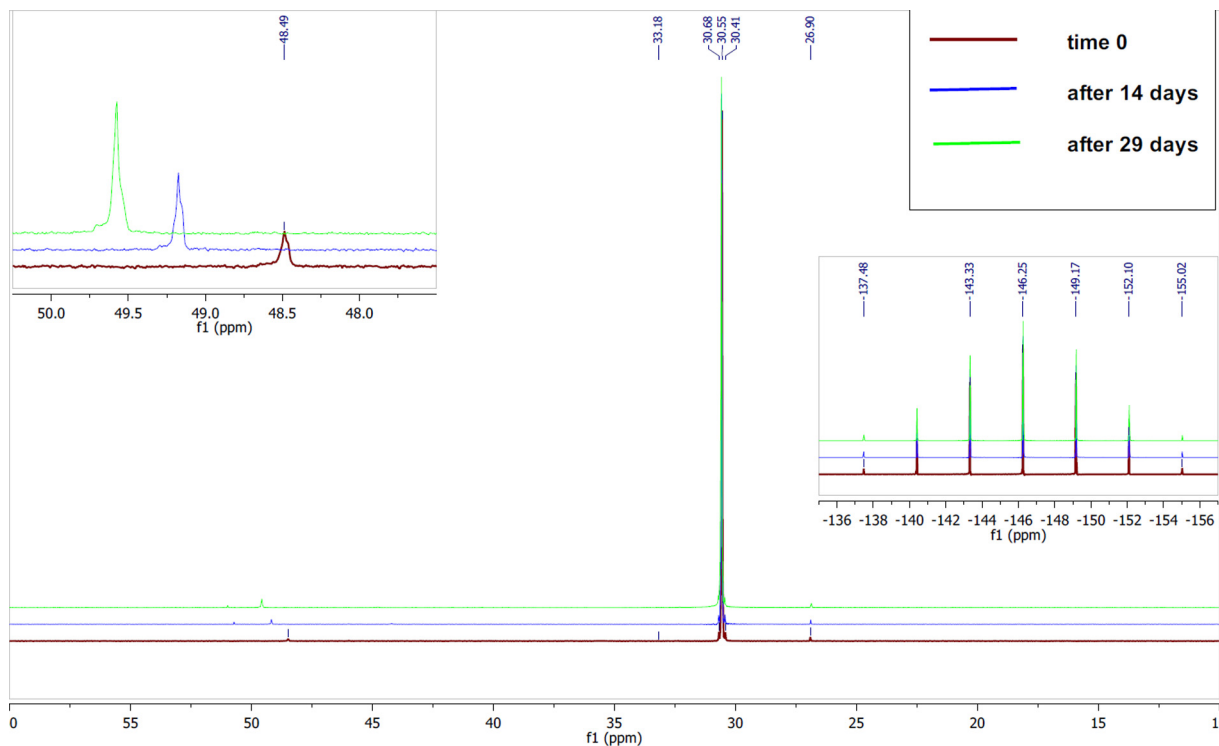


Fig. 6. P-31(¹H) NMR Spectra of **2**, (Oct)₃P=O (upper left) and HF (lower right) for 29 days.

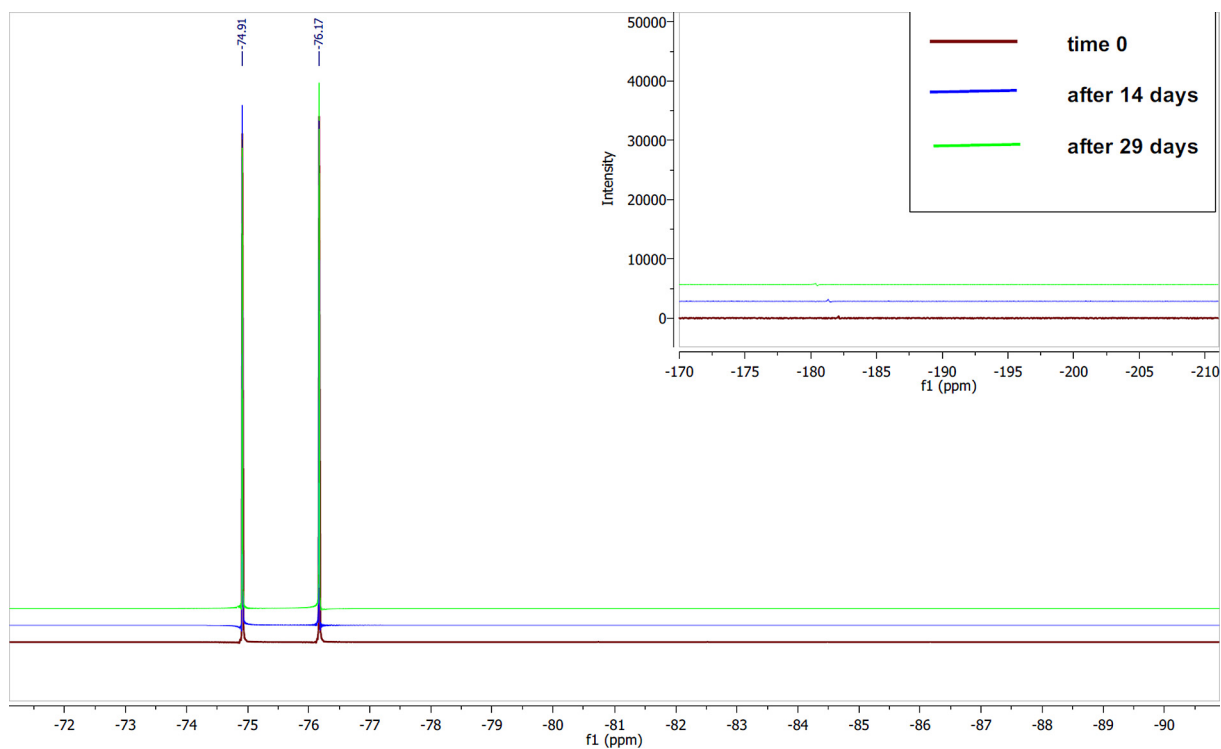


Fig. 7. F-19(¹H) NMR Spectra of **2** and HF (upper right) for 29 days.

Figs. 8, 10 and 12, the tight packing in **2** and **3** are also reflected in their closest interionic contacts. The other remarkable feature in **1** is the close proximity of the PF₆⁻ anion to one of the phenyl groups and imidazolium moiety with the associated C···P (C20···P2) interatomic distances of 3.121(2) Å. The most interesting feature of crystal packing in **2** is that the three octyl groups are staggered

and spread out laterally away from the ionic moieties. This open crystal packing among the octyl groups (between 8 and 13 Å) probably allows **2** to have a low melting point as observed in DSC measurements. Similar to the packing in **2**, compound **3** also exhibits tight packing of ions. The three C–N bond distances in all three PA's are comparable and fall between typical C–N single and dou-

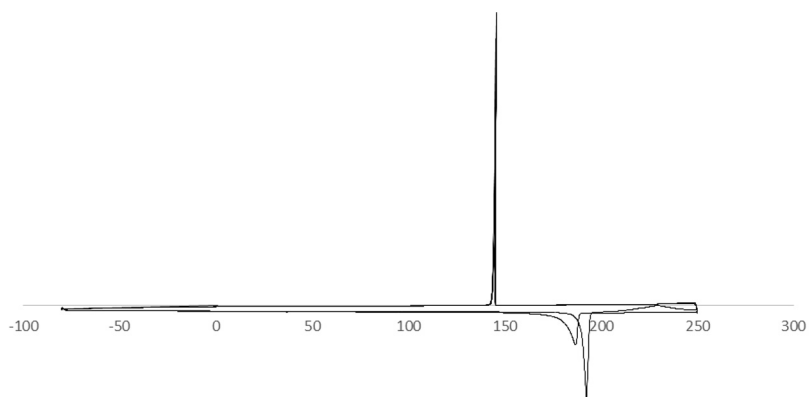


Fig. 8. DSC Trace of PA 1, two thermal cycles from –80 to 250 °C.

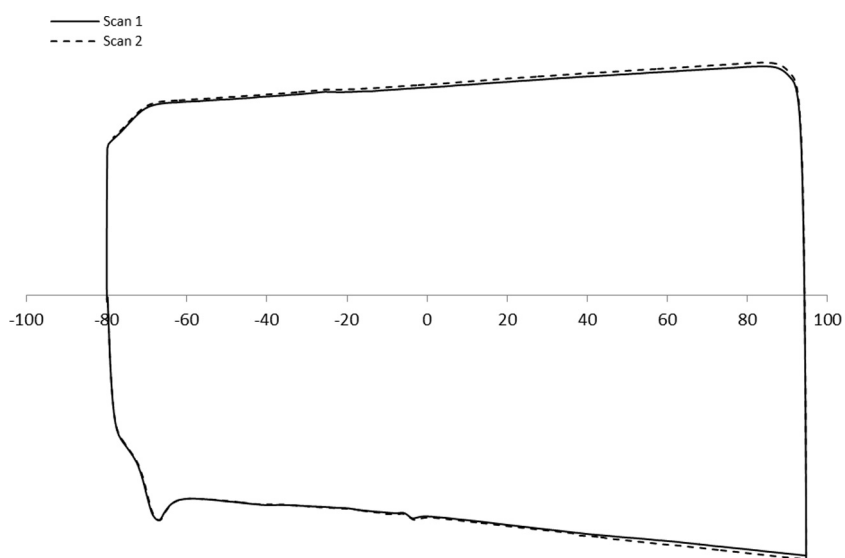


Fig. 9. DSC Trace of PA 2, two thermal cycles from –80 to 95 °C.

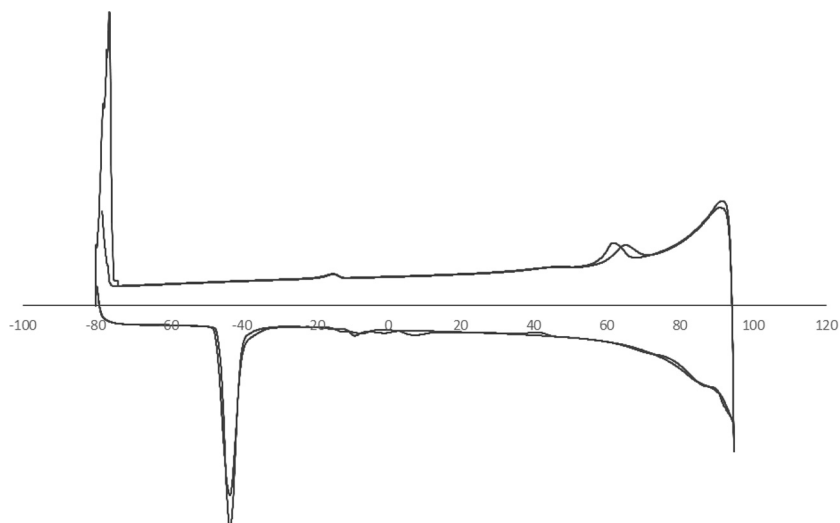
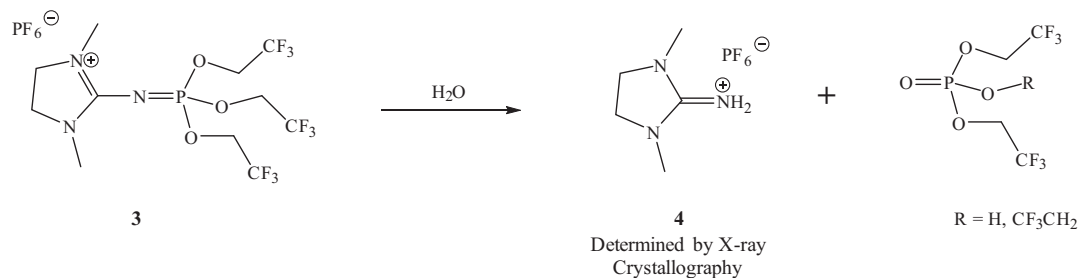


Fig. 10. DSC Trace of PA 3, two thermal cycles from –80 to 95 °C.

Scheme 2. Decomposition products of compound **3** after water exposure.Table 2
PA **1–3** crystallographic data.

Compound	1	2	3	4
Chemical formula	C ₂₃ H ₂₅ F ₆ N ₃ P ₂	C ₂₉ H ₆₀ F ₆ N ₃ P ₂	C ₁₁ H ₁₆ F ₁₅ N ₃ O ₃ P ₂	C ₅ H ₁₂ F ₆ N ₃ P
T, K	150	150	150	150
λ, Å	0.71073	0.71073	0.71073	0.71073
space group	P2 ₁ /c	P2 ₁ /c	P2 ₁ /c	P2 ₁ /n
a, Å	10.2614(2)	14.01775	9.3742(15)	8.1882(3)
b, Å	17.1198(3)	13.4151(5)	24.605(4)	11.3949(4)
c, Å	14.2207(3)	19.2683(7)	10.7300(16)	11.2514(4)
β, °	108.6855(10)	103.594(2)	115.470(9)	102.920(2)
V, Å ³	2366.52(8)	3521.9(2)	2234(6)	1023.22(6)
Z	4	4	4	4
D _{calc} , Mg m ⁻³	1.458	1.182	1.740	1.682
μ, mm ⁻¹	0.248	0.177	0.338	0.329
R1[I > 2σ(I)] ^a	0.416	0.0463	0.1600	0.0467
wR2[I > 2σ(I)] ^b	0.579	0.1165	0.2114	0.1394

^a R1 = $\sum ||F_o| - |F_c|| / \sum |F_o|$; ^b wR2 = $\{\sum [w(F_o^2 - F_c^2)^2] / \sum w(F_o^2)^2\}^{1/2}$.

Table 3
Selected bond distances (Å), bond angles (°) and torsion angles (°) for **1–4**.

Compound	1	2	3	4
P1–N1	1.5789(9)	1.5890(13)	1.501(6)	–
N1–C1	1.3100(13)	1.302(2)	1.323(8)	1.325(2)
C1–N2	1.3434(14)	1.342(2)	1.316(9)	1.327(2)
C1–N3	1.3569(13)	1.357(2)	1.316(9)	1.324(2)
P–C or P–O	1.7977(11)	1.7998(16)	1.551(6)	–
P–C or P–O	1.8001(11)	1.7981(16)	1.549(5)	–
P–C or P–O	1.8024(11)	1.8037(16)	1.599(6)	–
N1–C1–N2	130.33(10)	122.63(14)	121.1(8)	123.99(12)
N1–C1–N3	120.11(10)	128.13(14)	126.9(7)	124.42(13)
N2–C1–N3	109.56(9)	109.12(12)	112.0(6)	111.58(12)
P1–N1–C1	141.53(8)	140.42(12)	144.5(6)	–
P1–N1–C1–N2	3.6(2)	–135.2(2)	–118.8(11)	–
P1–N1–C1–N3	–175.7(1)	49.1(3)	64.2(14)	–

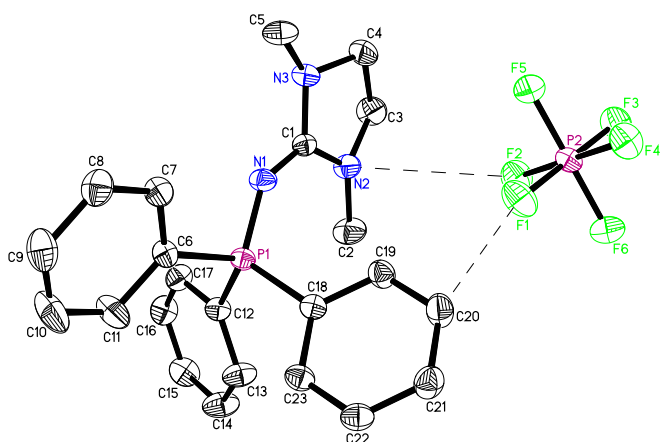


Fig. 11. View of the PA cation, **1** and the PF₆[−] anion. Hydrogen atoms are omitted. The broken lines represent the closest interionic contacts. The C...F and N...F distances are 3.121(1) and 3.456(1) Å, respectively.

ble bond distances (Table 2). The double bond across all three PA imidazolium is also nearly planar indicating possible delocalization of a double bond across the N2–C1–N3 units and potentially the lone pair on N1. The 2-amino-1,3-dimethylimidazolium cation present in **4** also exhibits similar double bond delocalization over the CN₃ unit (Table 2) and close proximity with the anion (Figs. 17 and 18). In addition, the C–N bond distances and N–C–N bond angles in the cation are similar to the corresponding distances in PA's **1–3** indicating that the P=N double bond present in the latter compounds do not significantly impact the nature of bonding within the dimethylimidazolium moiety.

From Table 4, the bond distances of a phosphorus–nitrogen bonds in an assortment of compounds can range from a P–N single bond at 1.78 Å to a P=N double bond at 1.54 Å [7,39–42,47]. Also in Table 4, various PA bond distances and bond angles measured in other studies are given along with the PA compounds **1–3** which are reported here; however, compound **4** is a decomposition product of **3**. Both ionic and neutral PAs included in the table display a variety of phosphonium (P–N) and phosphoranimine (P=N)

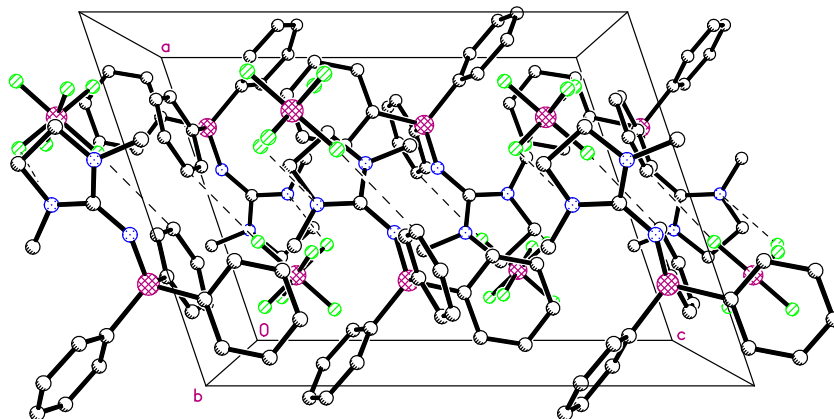


Fig. 12. Packing in the crystals of PA 1 as viewed along the b-axis. Hydrogen atoms are omitted and all atoms are unlabeled for clarity.

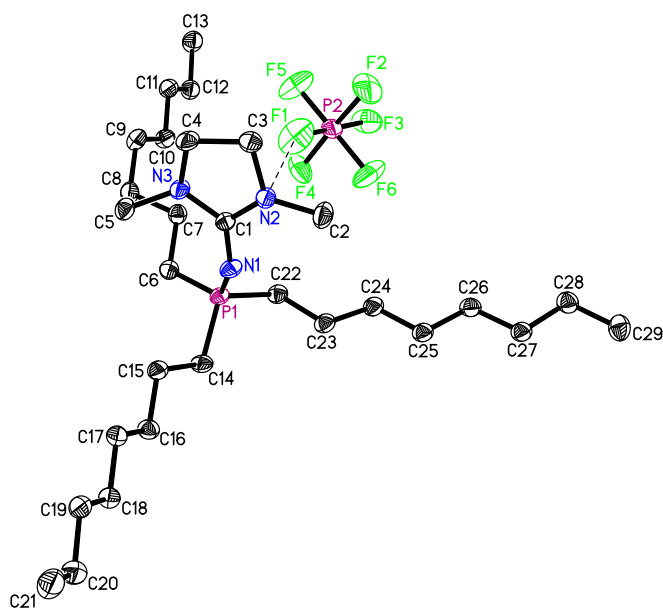


Fig. 13. View of the cation and anions in PA 2. Hydrogen atoms and the second set of sites for the four disordered F atoms of the anion are not shown. The broken line represents the shortest interionic distance. The N...F (N2...F1) distance is 3.163 (4) Å.

bond distances and angles. The interesting point is that the average P=N distance for phosphonium PA compounds [42] (Irmie) is about 1.63 Å and **1–2** are about 1.585 Å; however, the P=N distance for phosphonium PA compounds [39–41] (Huynh) and **3** have the shortest bond distances of ~1.50 Å. In all cases, the phosphonium PA salt P=N bond distances suggest a bond character between a single and double bond. The closest representative single bond phosphonium bond is with Irmie et al.'s compounds [42]. The bond distance differences between the ionic and neutral forms of PA compounds are not substantial; however they reside closer to a double bond than a single bond in most cases. Therefore, it suggests that the positive charge remains delocalized rather than localized on a single atom.

The R–N=P bond angles on these compounds show interesting trends, and the Huynh et al.'s PAs and PAs **1–3** have a large bond angle that is greater than 140° (more linear). The Me₃Si-group contributes back π -orbital overlap to give a linear R–N=P bond angle, which is shown with Huynh et al.'s PA compounds with large bond

angles from 144° to 166° and Me₃Si–N=PPh₃ at 138°. This suggests that the imidazolium group is interacting R–N=P bond to give **1–3** larger bond angles. However, Irmie et al.'s PA compounds show smaller bond angles at around 125°, which is caused by the substituted nitrogen and forcing the R–N=P to be bent. Again, these bond angles and bond distances could be influenced by crystal packing, but there are some trends that are different from other PA compounds.

3. Conclusions

Three new PA salts were formed by the Staudinger reaction using an ionic azide, ADMImPF₆. The reaction is straightforward in making the respective ionic PA products; however, these PA products tend not to be soluble in toluene, hexanes or water. It is interesting that the isolated PA **1–2** salts are not extremely reactive to air or moisture; however, the isolated PA **3** salt decomposes upon exposure to the atmosphere. The remarkable feature of these compounds is that **2** is an ionic liquid at room temperature. From P-31 and F-19 NMR, the spectra show that PAs **1–2** are stable towards water laden organic solvents for extended periods without noticeable degradation products. In addition, thermal cycling of **1–3** by DSC shows that **1** and **2** are stable to 90 °C, but **3** decomposes into its corresponding phosphine oxide and DMImPF₆ after one thermal cycle. The X-ray structure data of **1–3** reveal that the PF₆[−] anion resides nearby the imidazolium functional group. Also from the X-ray, crystals of **2** have an open packing structure which can explain its RTIL behavior (m.p. −5 °C). When comparing the X-ray structures of other known ionic PA compounds, it can be seen that the imidazolium interacts with the P=N bond resulting in larger than 140° bond angle at R'–N=P. Overall, **1–3** are easily synthesized to form N-substituted ionic PA compounds without noted complications commonly found using the Staudinger reaction.

4. Experimental section

4.1. Materials and general procedures

The following reagents were obtained from commercial sources and used without further purification: 2-Azido-1,3-dimethylimidazolium hexafluorophosphate (ADMImPF₆; Aldrich), triphenylphosphine (TPP; Aldrich), tris(2,2,2-trifluoroethoxy)phosphite (TTFP; Strem) and tri-*n*-octylphosphine (TOP; Strem). House deionized (DI) water was purified by a Millipore 302 system that achieved an 18 MOhm rating and used directly. Anhydrous solvents, such as toluene, tetrahydrofuran (THF) and hexane were

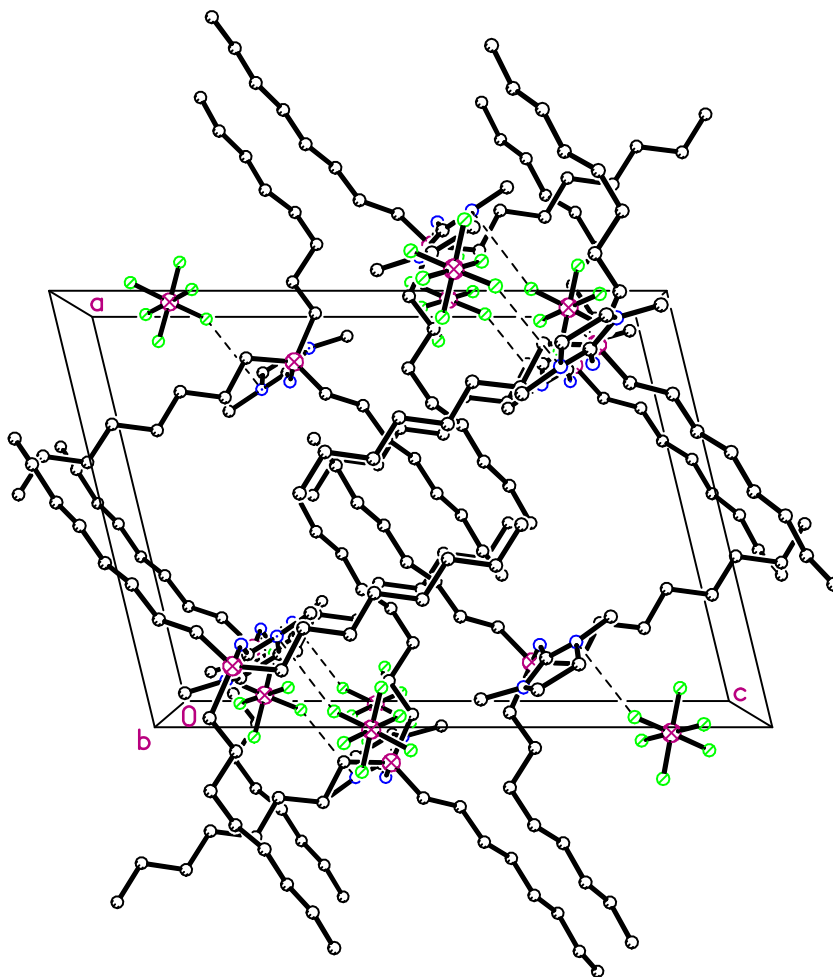


Fig. 14. Packing in the crystals of PA **2**, a as viewed along the b-axis. Hydrogen atoms and the second set of sites for the four disordered F atoms of the anion are not shown and all atoms are unlabeled.

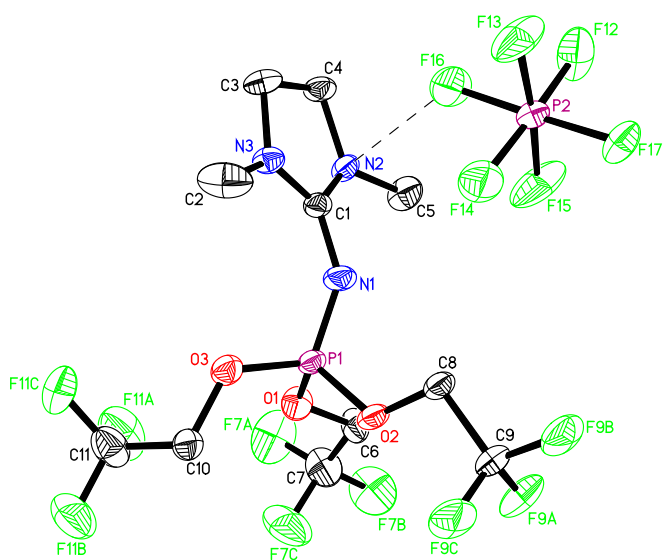


Fig. 15. View of the cation and anion in PA **3**. Hydrogen atoms and the second set of sites for the four disordered F atoms of the anion are not shown. The broken line represents the shortest interionic contact. The N...F (N2...F16) distance is 3.273(9) Å.

obtained from Aldrich and used as received. Proton, $^{13}\text{C}\{^1\text{H}\}$, $^{19}\text{F}\{^1\text{H}\}$ and $^{31}\text{P}\{^1\text{H}\}$ Nuclear Magnetic Resonance (NMR) spectra were recorded on a Bruker Ascend Avance III 600 MHz spectrometer. MNOVA NMR software package (v10.0.2) was used for multiple NMR spectra arrangements [51].

4.2. $^{19}\text{F}\{^1\text{H}\}$ and $^{31}\text{P}\{^1\text{H}\}$ NMR moisture exposure experiments

NMR-based moisture exposure experiments were conducted on PA compounds, **1** and **2**, over a 29 day time frame. The solutions were made with 0.2–0.25 g of PA in 1 mL of d_8 -THF (Cambridge Isotopes) containing 10 wt% water (by solvent) in each NMR sample tube. A polypropylene cap was used on the NMR tubes for the duration of these experiments. $^{19}\text{F}\{^1\text{H}\}$ and $^{31}\text{P}\{^1\text{H}\}$ NMR spectra were periodically recorded to observed spectral changes in the hexafluorophosphate and the PA compounds.

4.3. Differential Scanning Calorimetry (DSC) data

Thermal analysis was obtained using a TA Instruments (New-Castle, DE) model Q200 Differential Scanning Calorimeter (DSC). For data collection, T_{zero} aluminum hermetic pans were loaded with ~10 mg of sample and the temperature was cycled between –80 and 250 °C at a rate of 5 °C, under a purge gas (N_2) with a flow

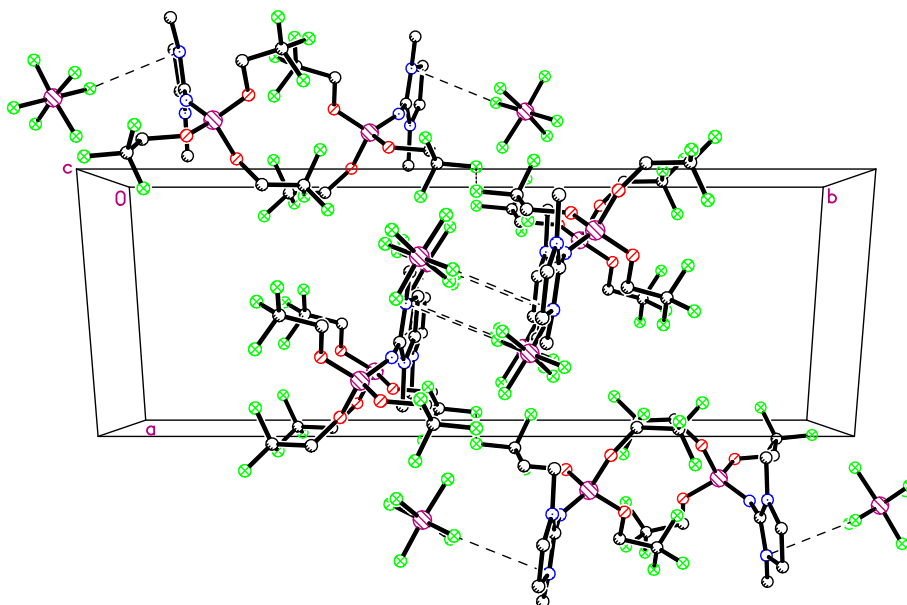


Fig. 16. Packing in the crystals of PA 3, a as viewed along the b-axis. Hydrogen atoms and the second set of sites for the four disordered F atoms of the anion are not shown. All atoms are unlabeled for clarity.

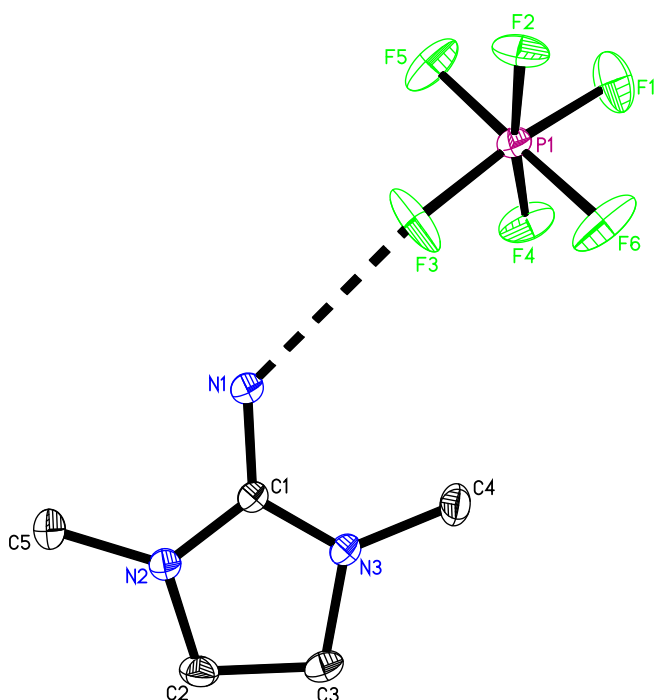


Fig. 17. View of the cation and anion in **4**. Hydrogen atoms and the second set of sites for the four disordered F atoms of the anion are not shown. The broken line represents the shortest interionic contact. The N...F (N1...F3) distance is 2.841(6) Å.

rate of 50.0 mL/min. Before cycling, the temperature was held at $-80\text{ }^{\circ}\text{C}$ to ensure complete equilibration.

4.4. Crystallographic data

The X-ray diffraction data for **1–4** were measured at 150 K on a Bruker SMART APEX II CCD area detector system equipped with a graphite monochromator and a Mo $K\alpha$ fine-focus sealed tube operated at 1.5 kW power (50 kV, 30 mA). Colorless crystals were glued to a glass fiber using Paratone N oil and the detector was placed at

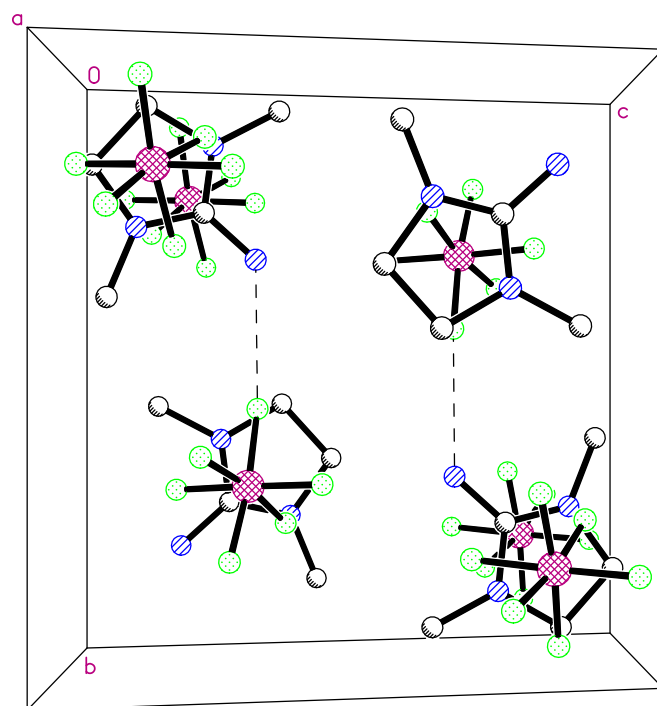


Fig. 18. Packing in the crystals of **4**, as viewed along the a-axis. Hydrogen atoms and the second set of sites for the four disordered F atoms of the anion are not shown. All atoms are unlabeled for clarity.

a distance of 5.13 cm from the crystal during the data collection. A series of narrow frames of data were collected with a scan width of 0.5° in ω or ϕ and an exposure time of 20 s per frame. The frames were integrated with the Bruker SAINT Software package¹ using a narrow-frame integration algorithm. The data were corrected for absorption effects by the multi-scan method (SADABS). Crystallographic data collection parameters and refinement data are collected below in Table 1. Structures were solved by the direct methods using the Bruker SHELXTL (V. 2014.11-0) Software Package [52].

Table 4
Bond distances and bond angles from X-ray crystal determination data on various phosphoranimines along with PAs 1–3.

Phosphoranimine	Bond distances (Å)			Bond angle (°)
	C–P	P=N	N–R'	P=N–R'
[1] ^a	1.800(1)	1.579(1)	1.337(11)	141.53(8)
[2] ^a	1.800(2)	1.589(1)	1.334(2)	140.42(12)
[3] ^a	1.566(6)	1.501(6)	1.318(9)	144.5(6)
Ph–N=PPh ₃ ^b	1.808	1.603	1.329	130.4
Me ₃ Si–N=PPh ₃ ^c	1.818	1.547	1.692	138.4
[Ph ₃ P=N=PPh ₃] ⁺ Cl ^{–d}	1.795	1.598	–	133.1
[iPr–N(H)=PPh ₃] ⁺ Br ^{–e}	1.784	1.628	–	124.2
[tBu–N(H)=PPh ₃] ⁺ Br ^{–e}	1.800	1.621	–	129.1
[tBu–N(Me)=PPh ₃] ⁺ I ^{–e}	1.800	1.646	–	121.3
[Me ₃ SiN=P(OCH ₂ CF ₃) ₂ ← DMAP] ⁺ BF ₄ ^f	–	1.489	1.690	166.0
[Me ₃ SiN=P(OCH ₂ CF ₃) ₂ ← PEt ₃] ⁺ Br ^{–g}	–	1.492	1.722	158.1
[Me ₃ SiN=P(OCH ₂ CF ₃) ₂ ← PMe ₃] ⁺ Br ^{–g}	–	1.479	1.694	160.9
[Me ₃ SiN=PMe ₂ ← PEt ₃] ⁺ CF ₃ SO ₃ ^{–g}	1.793	1.508	1.671	154.0
[Me ₃ SiN=PMe ₂ ← PMe ₃] ⁺ Br ^{–g}	1.792	1.533	1.696	144.0

^a This work.

^b Ref. [48].

^c Ref. [49].

^d Ref. [50].

^e Ref. [42].

^f Ref. [40].

^g Ref. [41].

All non-hydrogen atoms were located in successive Fourier maps and refined anisotropically. The PF₆[–] anion in **1** is well ordered, whereas those in **2–4** are disordered. The disorder in **2** and **4** is modeled by assigning two sites for all of the F atoms and refining their site occupancies with a free variable. The two sets of F atoms in **2** and **4** settle on occupancies of 64 and 36%, and 57 and 43%, respectively, leading to satisfactory overall refinement of the structures. The disorder in **3** is modeled by assigning two sets of sites for four of the F atoms. A free variable refinement of their site occupancies settle on 61 and 39%. The overall refinement of this structure is poor owing to the poor diffraction of the crystals. However, the structural parameters deduced are of sufficient quality. All hydrogen atoms were located and refined isotropically in the structures of **1**, **2** and **4**. The hydrogen atoms were placed in calculated positions for **3** and refined isotropically with fixed thermal parameters adapting a riding model.

4.5. Synthesis of P,P,P-triphenylphosphoraniminyl-N-1,3-dimethylimidazolium hexafluorophosphate, (**1**)

A 50 mL two-necked, round bottom flask was equipped with a water condenser, gas inlet, magnetic stir bar, and a rubber septum was purged with nitrogen. 10 mL of anhydrous toluene was introduced into the flask by syringe, and then ADMImPF (2.0 g, 0.007 mol) was added directly into the flask. The azide has limited solubility in toluene which makes a slurry. TPP (1.9 g, 0.007 mol) is dissolve in 10 mL of anhydrous toluene and the solution was added dropwise by syringe into the flask. As the phosphine addition progressed, an intense yellow color was observed during the reaction. Off gassing of nitrogen is observed as the reaction was heated to reflux. The reaction was refluxed with monitoring for one hour and then allowed to reflux overnight under nitrogen. The yellow color subsided as the reaction was refluxed overnight. The reaction then was allowed to cool to room temperature, where the desired compound precipitated as a white solid. Excess toluene was removed and the product was washed twice with 30–40 mL of hexanes. The white solid was collected and re-crystallized in tetrahydrofuran. The product showed no degradation in ambient atmosphere and upon exposure to water at room temperature. [87% yield, m.p. = 185 °C, ³¹P NMR δ (d₆-Acetone) = (s) 13.0, (septet, J_{PF} = 707.0 Hz) –144.2; ¹⁹F NMR δ (d₆-Acetone) = (d, J_{PF} = 706.0 Hz) –72.6; ¹H NMR δ (d₆-Acetone) = (m) 7.81–7.90, (m) 7.73, (s) 3.70,

(s) 2.78; ¹³C NMR δ (d₆-Acetone) = (s) 133.7, (d, J_{PC} = 10.6 Hz) 132.4, (d, J_{PC} = 12.1 Hz) 129.7, (d, J_{PC} = 107.2 Hz) 128.3, (s) 47.0, (s) 33.2].

4.6. Synthesis of P,P,P-tri-n-octylphosphoraniminyl-N-1,3-dimethylimidazolium hexafluorophosphate, (**2**)

A 50 mL two-necked, round bottom flask, water condenser equipped with a gas inlet, magnetic stir bar, and a rubber septum was purged with nitrogen. 10 mL of anhydrous toluene was introduced into the flask by syringe, and then ADMImPF (2.0 g, 0.007 mol) was added directly into the flask. The azide has limited solubility in toluene which makes a slurry. TOP (3.12 mL, 2.6 g, 0.007 mol) was added dropwise by syringe into the flask. As the phosphine addition progressed, an intense yellow color was observed during the reaction resulting is a yellow slurry. 20–30 min after the phosphine was added, the yellow color subsided and the reaction was heated to near reflux. No apparent nitrogen off-gassing was observed as the reaction was heated to reflux. The reaction then was refluxed overnight under nitrogen. Next day, the reaction was allowed to cool to room temperature. Stirring was stopped and no phase separation was observed. The reaction solution was filtered, collected and toluene was removed by a flowing nitrogen gas stream. The product was washed thrice with 30–40 mL of hexanes, and the remaining hexanes were removed from bottom phase by a flowing nitrogen stream. The concentrate was dissolved in toluene where the remaining solids were allowed to settle and the remaining solution was removed and concentrated by a flowing nitrogen stream. The resulting product is a clear, colorless liquid. The product was stable in air and remains a liquid at room temperature. The purified product slowly crystallizes in a freezer at –30 °C to yield colorless, clear prismatic crystals. [73% yield, m.p. = –5 °C, viscosity = 740 cP at 25.5 °C, ³¹P NMR δ (d₆-Acetone) = (s) 32.5, (septet, J_{PF} = 707.0 Hz) –144.3; ¹⁹F NMR δ (d₆-Acetone) = (d, J_{PF} = 706.0 Hz) –72.6; ¹H NMR δ (d₆-Acetone) = (s) 3.66, (s) 2.98, (doublet of triplets, J_{PH} = 6.0 Hz, J_{HH} = 8.4 Hz) 2.24, (doublet of pentets, J_{PH} = 7.8 Hz, J_{HH} = 7.8 Hz) 1.70, (pentet, J_{HH} = 7.8 Hz) 1.70, (m) 1.28–1.42, (m) 3.45–3.51, (t, J_{HH} = 7.8 Hz) 0.90; ¹³C NMR δ (d₆-Acetone) = (s) 46.7, (s) 32.9, (s) 31.6, (d, J_{PC} = 15.1 Hz) 30.5, (m) 28.8, (d, J_{PC} = 63.4 Hz) 27.0, (s) 22.4, (s) 21.6, (s) 13.4].

4.7. Synthesis of P,P,P-tris(2,2,2-trifluoroethoxy)phosphoraniminyl-N-1,3-dimethylimidazolium hexafluorophosphate, (**3**)

Following the procedure as for **PA 2**, 10 mL of anhydrous toluene was introduced into the flask by syringe, and then ADMImPF (2.0 g, 0.007 mol) was added directly into the flask. TTFP (1.54 mL, 2.3 g, 0.007 mol) was added dropwise by syringe into the flask. As the phosphine addition progressed, no color was observed during the reaction but remains as a slurry. 20–30 min after the phosphine was added, no color was observed during the reaction. No apparent off gassing (nitrogen) is observed and the reaction was left at room temperature overnight under nitrogen. Next day, stirring was stopped and the white, powdery product was allowed to settle. The product was collected by decanting the toluene and the product was washed twice with 30–40 mL of hexanes. The powdery solids were dried by a nitrogen gas stream overnight. The isolated product is moderately stable in air from days to weeks depending on humidity. The product was recrystallized in boiling THF, and it is allowed to slowly cool to room temperature. The final product forms colorless, clear prismatic crystals. However, long-term stability of **3** was an issue after exposure to moisture, and **4** is the decomposition product of **3**. [85% yield, m.p. = 97–98 °C, ^{31}P NMR δ (d_6 -Acetone) = (s) -14.8, (septet, $J_{\text{PF}} = 707.0$ Hz) -144.3; ^{19}F NMR δ (d_6 -Acetone) = (d, $J_{\text{PF}} = 711.4$ Hz) -72.6, (s) -75.7; ^1H NMR δ (d_6 -Acetone) = (quartets, $J_{\text{HF}} = 7.8$ Hz) 5.11, (s) 3.83, (s) 3.09; ^{13}C NMR δ (d_6 -Acetone) = (d, $J_{\text{PC}} = 22.7$ Hz) 156.0, (q, $J_{\text{CF}} = 274.8$ Hz) 122.4, (d, $J_{\text{PC}} = 7.6$ Hz, $J_{\text{CF}} = 31.7$ Hz) 30.5, (s) 47.2, (s) 32.2].

Acknowledgements

Work supported through the Idaho National Laboratory - Laboratory Directed Research and Development (LDRD) Program, Project 15-125, under United States - Department of Energy (USDOE) Idaho Operations Office (Contract No. DE-AC07-05ID14517). This manuscript has been authored by Battelle Energy Alliance, LLC under Contract No. DE-AC07-05ID14517 with the U.S. Department of Energy. The United States Government retains and the publisher, by accepting the article for publication, acknowledges that the United States Government retains a nonexclusive, paid-up, irrevocable, world-wide license to publish or reproduce the published form of this manuscript, or allow others to do so, for United States Government purposes.

References

- [1] C.W. Allen, *Coord. Chem. Rev.* 130 (1994) 137–173.
- [2] P. Potin, R. De Jaeger, *Eur. Polym. J.* 27 (1991) 341–348.
- [3] R.H. Neilson, P. Wisian-Neilson, *Chem. Rev. Wash. DC U. S.* 88 (1988) 541–562.
- [4] H.R. Allcock, F.W. Lampe, *Contemporary Polymer Chemistry*, Prentice-Hall, 1981.
- [5] A.K. Andrianov, *Polyphosphazenes for Biomedical Applications*, John Wiley and Sons, 2009.
- [6] M. Carenza, S. Lora, L. Fambri, in: N. Hasirci, V. Hasirci (Eds.), *Biomaterials*, Springer, US, 2004, pp. 113–122.
- [7] M. Gleria, R.D. Jaeger, *Phosphazenes: A Worldwide Insight*, Nova Publishers, 2004.
- [8] R.D. Jaeger, M. Gleria, *Applicative Aspects of Poly(organophosphazenes)*, Nova Publishers, 2004.
- [9] E.J. Dufek, J.R. Klaehn, J.S. McNally, H.W. Rollins, D.K. Jamison, *Electrochim. Acta* 209 (2016) 36–43.
- [10] P. Wisian-Neilson, in: R.B. King (Ed.), *Encycl. Inorg. Chem.*, 1st ed., John Wiley & Sons, Chichester, England, 1994, pp. 3371–3384.
- [11] Y.G. Gololobov, L.F. Kasukhin, *Tetrahedron* 48 (1992) 1353–1406.
- [12] P. Wisian-Neilson, R.H. Neilson, *J. Am. Chem. Soc.* 102 (1980) 2848–2849.
- [13] C.H. Honeyman, I. Manners, C.T. Morrissey, H.R. Allcock, *J. Am. Chem. Soc.* 117 (1995) 7035–7036.
- [14] H.R. Allcock, C.A. Crane, C.T. Morrissey, J.M. Nelson, S.D. Reeves, C.H. Honeyman, I. Manners, *Macromolecules* 29 (1996) 7740–7747.
- [15] V. Blackstone, A.J. Lough, M. Murray, I. Manners, *J. Am. Chem. Soc.* 131 (2009) 3658–3667.
- [16] V. Blackstone, S. Pfirrmann, H. Helten, A. Staubitz, A. Presa Soto, G.R. Whittell, I. Manners, *J. Am. Chem. Soc.* 134 (2012) 15293–15296.
- [17] V. Vreeken, M.A. Siegler, B. de Bruin, J.N.H. Reek, M. Lutz, J.I. van der Lugt, *Angew. Chem. Int. Ed.* 54 (2015) 7055–7059.
- [18] A. Steiner, S. Zacchini, P.I. Richards, *Coord. Chem. Rev.* 227 (2002) 193–216.
- [19] D.W. Stephan, J.C. Stewart, F. Guerin, S. Courtenay, J. Kickham, E. Hollink, C. Beddie, A. Hoskin, T. Graham, P. Wei, R.E.V. H. Spence, W. Xu, L. Koch, X. Gao, D. G. Harrison, *Organometallics* 22 (2003) 1937–1947.
- [20] M.A. Benson, J. Ledger, A. Steiner, *Chem. Commun.* (2007) 3823–3825.
- [21] F. Dielmann, C.E. Moore, A.L. Rheingold, G. Bertrand, *J. Am. Chem. Soc.* 135 (2013) 14071–14073.
- [22] N. Burford, T.S. Cameron, D.J. LeBlanc, A.D. Phillips, T.E. Concolino, K.-C. Lam, A. L. Rheingold, *J. Am. Chem. Soc.* 122 (2000) 5413–5414.
- [23] R. Boomishankar, J. Ledger, J.-B. Guilbaud, N.L. Campbell, J. Bacsá, R. Bonar-Law, Y.Z. Khimyak, A. Steiner, *Chem. Commun.* (2007) 5152–5154.
- [24] O. Alhomaïdan, G. Bai, D.W. Stephan, *Organometallics* 27 (2008) 6343–6352.
- [25] N.J. Van Zee, M.J. Sanford, G.W. Coates, *J. Am. Chem. Soc.* 138 (2016) 2755–2761.
- [26] J.K. Ruff, W.J. Schlientz, R.E. Dessy, J.M. Malm, G.R. Dobson, M.N. Memering, in: G.W. Parshall (Ed.), *Inorg. Synth.*, Wiley & Sons Inc, John, 1974, pp. 84–90.
- [27] R.H. Neilson, J.R. Klaehn, *J. Inorg. Organomet. Polym. Mater.* 16 (2006) 319–326.
- [28] J.R. Klaehn, R.H. Neilson, *Inorg. Chem.* 41 (2002) 5859–5865.
- [29] H. Staudinger, J. Meyer, *Helv. Chim. Acta* 2 (1919) 619–635.
- [30] K. Matyjaszewski, M.S. Lindenberg, M.K. Moore, M.L. White, *J. Polym. Sci. Part Polym. Chem.* 32 (1994) 465–473.
- [31] J. Haase, in: S. Bräse, K. Banert (Eds.), *Org Azides*, John Wiley & Sons Ltd, 2009, pp. 29–51.
- [32] H.C. Kolb, M.G. Finn, K.B. Sharpless, *Angew. Chem. Int. Ed.* 40 (2001) 2004–2021.
- [33] V. Hong, N.F. Steinmetz, M. Manchester, M.G. Finn, *Bioconjug. Chem.* 21 (2010) 1912–1916.
- [34] H. Yoon, J.M. Lim, H.-C. Gee, C.-H. Lee, Y.-H. Jeong, D. Kim, W.-D. Jang, *J. Am. Chem. Soc.* 136 (2014) 1672–1679.
- [35] F. Shabanpoor, M.J. Gait, *Chem. Commun.* 49 (2013) 10260–10262.
- [36] M. Kitamura, T. Koga, M. Yano, T. Okauchi, *Synlett* 23 (2012) 1335–1338.
- [37] M. Kitamura, S. Kato, M. Yano, N. Tashiro, Y. Shiratake, M. Sando, T. Okauchi, *Org. Biomol. Chem.* 12 (2014) 4397–4406.
- [38] M. Kitamura, M. Yano, N. Tashiro, S. Miyagawa, M. Sando, T. Okauchi, *Eur. J. Org. Chem.* 2011 (2011) 458–462.
- [39] K. Huynh, C.P. Chun, A.J. Lough, I. Manners, *Dalton Trans.* 40 (2011) 10576–10584.
- [40] K. Huynh, E. Rivard, A.J. Lough, I. Manners, *Chem. Eur. J.* 13 (2007) 3431–3440.
- [41] K. Huynh, A.J. Lough, M.A.M. Forgeron, M. Bendle, A.P. Soto, R.E. Wasylshen, I. Manners, *J. Am. Chem. Soc.* 131 (2009) 7905–7916.
- [42] C. Imrie, T.A. Modro, P.H. Van Rooyen, C.C.P. Wagener, K. Wallace, H.R. Hudson, M. McPartlin, J.B. Nasirun, L. Powroznik, *J. Phys. Org. Chem.* 8 (1995) 41–46.
- [43] H. Zimmer, G. Singh, *J. Org. Chem.* 28 (1963) 483–486.
- [44] S.P. Belov, I.V. Komlev, S.V. Kuznetsov, E.E. Nifant'ev, *Russ. J. Gen. Chem.* 79 (2009) 2698–2699.
- [45] T.W. Rave, *J. Org. Chem.* 32 (1967) 3461–3466.
- [46] L. Maier, P.J. Diel, *Phosphorus Sulfur Silicon Relat. Elem.* 115 (1996) 273.
- [47] I. Alkorta, G. Sánchez-Sanz, J. Elguero, J.E. Del Bene, *J. Phys. Chem. A* 118 (2014) 1527–1537.
- [48] M.H. Holthausen, I. Mallov, D.W. Stephan, *Dalton Trans.* 43 (2014) 15201–15211.
- [49] F. Weller, H.-C. Kang, W. Massa, T. Rübenthal, F. Kunkel, Kurt Dehnicke, *Z. Naturforsch.* 50b (1995) 1050–1054.
- [50] C. Knapp, R. Uzun, *Acta Crystallogr. Sect. E Struct. Rep. Online* 66 (2010). o3185–o3185.
- [51] MNova NMR, V. 10.0.2, Mestrelab Research S.L., Feliciano Barrera, Spain, 2016.
- [52] APEX2 Software Suite V. 2014.11-0, Bruker AXS Inc., Madison, WI, 2014.